NARROW BRANCH PRESERVATION IN MORPHOLOGICAL RECONSTRUCTION

Kevin Robinson* and Paul F. Whelan
Vision Systems Group
Dublin City University, Ireland

Abstract

We present a morphological approach to the reconstruction of fine branching structures in three dimensional data, developed from the basic procedures of reconstruction by dilation. We address a number of closely related questions arising from this reconstruction goal, including issues of structuring element size and shape, noise propagation, iterated approaches, and the relationship between geodesic and conditional dilation. We investigate and assess the effect and importance of these considerations in the context of the overall reconstruction process, and examine the effectiveness of the approach in addressing the task of reconstructing narrow branch features in noisy data.
Keywords*: Mathematical morphology, Reconstruction by dilation, Structuring element, Geodesic dilation, Conditional dilation*

1 Introduction

The classical reconstruction by dilation procedure [8, 10] is an effective and much utilised image processing tool applied extensively in the segmentation and classification of complex scenes [1, 2, 4, 6]. Seeded regions are retained while neighbouring unseeded regions are attenuated to the intensity level of the surrounding background data. The approach yields excellent results in isolating compact regions in noisy data. However when the regions of interest include fine branching structures the approach performs less well, especially in the presence of noise. This behaviour is due to the geodesic growth properties at the heart of the definition of reconstruction by dilation. The geodesic dilations which constitute a reconstruction by dilation guarantee that there exists a connected, strictly uphill (in terms of pixel intensity) path from each sample point to one of the original set of seed points which initiated the procedure. This property is what achieves the suppression of non-seeded high intensity regions.

The difficulty arises when a narrow element is encountered in a seeded region. Any signal drop-off along the narrow branch (due to noise or transitory signal reduction) can result in an undesirable attenuation of the intensity level along the entire remainder of the branch length. This is not an issue in the reconstruction of more compact regions as there will exist some convoluted high intensity path to carry the signal past the blockage. As the features in the region to be reconstructed become more and more narrow the chances of encountering a signal drop-off which can not be negotiated at the higher signal intensity level increase. In the case of fine branches, where the high intensity path is only one or two pixels wide the likelihood of undesirable signal suppression becomes extreme, leading to incomplete reconstruction of the desired objects.

In order to counter this difficulty we propose a non-geodesic extension to the reconstruction by dilation procedure aimed at bridging small gaps in the high intensity path while still effectively suppressing the signal intensity in neighbouring regions. The approach has the additional desirable property of preserving

*Corresponding author. *E-mail address:* kevin.robinson@eeng.dcu.ie

more fully the textural information in the reconstructed regions and suppressing the stepped contour effects which otherwise often manifest. These properties can be beneficial in terms of both the analysis and visualisation of the processed data.

The motivation for this work stems from a project whose aim is the segmentation of a ductal system called the biliary tree from a class of medical MRI scans of the abdomen. See Figure 1 for a maximum intensity projection (MIP) rendering of the three dimensional data from one such MRI scan. The ductal tree is clearly visible along with a number of occluding high intensity structures which we wish to suppress. Successful isolation of the finer branches towards the periphery of the tree is highly dependant on suppression of the high intensity proximal structures in the scene.

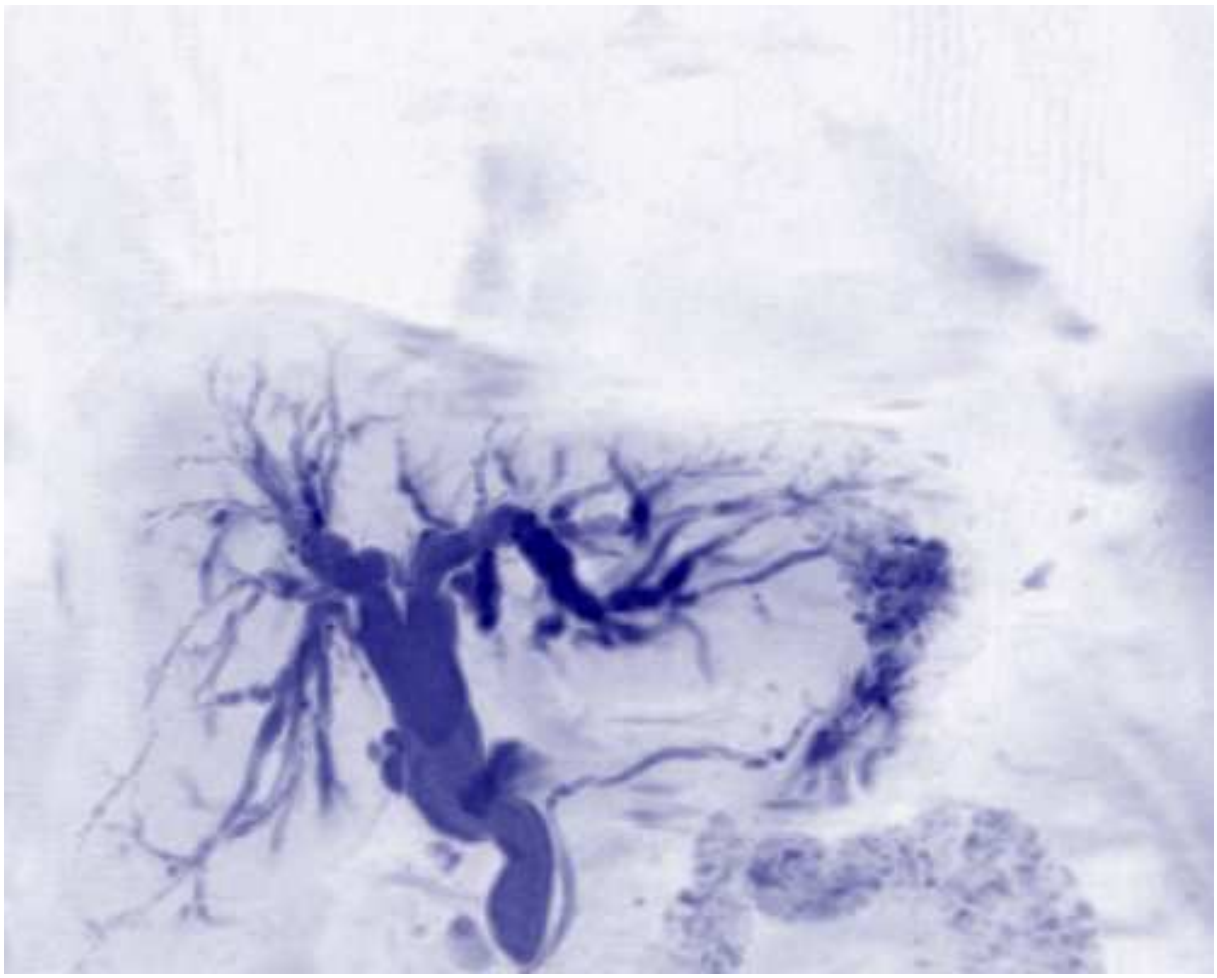

Figure 1: Illustration of the ductal tree whose segmentation is the ultimate goal. Neighbouring high intensity structures complicate the task.

2 Method

2.1 Morphological dilation operators

We first review the definitions of and the differences between dilation, conditional dilation, and geodesic dilation in greyscale data [7, 8]. Standard greyscale morphological dilation, $\delta^{(N)}$ is achieved where each sample point in the output is set equal to the maximum of it's own input intensity value and the values of

all sample points within a given neighbourhood in the source:

$$\delta^{(N)} I \;\widehat{=}\; \forall p : D \bullet \forall q : N_G(p) \bullet (q \leftarrow max(p, q)) \tag{1}$$

where D is the image domain and N signifies the 'size' of the dilation, represented in terms of N_G, the set of neighbouring samples constituting the structuring element to be applied in the dilation. Thus we can say, for all sample points p in the domain, for all sample points q in the neighbourhood of p, the output at q becomes the larger of p and q.

Conditional ($\delta_C^{\star(N)}$) and geodesic ($\delta_C^{(N)}$) dilations are then easily defined in terms of standard dilation as shown in Eqs. 2 and 3 respectively, where C represents the conditioning dataset, which must share the same domain as I, and $\wedge$ is the point-wise minimum operator.

$$\delta_C^{\star(N)} I \;\widehat{=}\; \delta^{(N)} I \wedge C \tag{2}$$

$$\delta_C^{(N)} I \;\widehat{=}\; \delta^{(1)} I \wedge C \ldots N \; times \tag{3}$$

Thus we can see that while in conditional dilation the point-wise minimum is applied only once after dilation to the full extent specified has been achieved, in geodesic dilation it is applied after each application of the fundamental dilation operator, with the two steps being repeated the necessary number of times. By applying the minimum at each iteration the procedure limits the growth of the dilated areas so as to avoid jumping over low intensity background regions in the conditioning mask and growing into unseeded neighbouring high intensity regions.

This behaviour is illustrated in Figure 2, where fig2c shows the standard (unconditional) dilation iterated until stability, which results in the entire domain arriving at the intensity level of the brightest sample point present in the marker (fig2a). Fig2d illustrates that the only difference between conditional dilation iterated until stability and the conditioning mask used to generate it, (fig2b) is that all sample points in the mask of a higher intensity than the highest intensity sample point in the marker have been capped at that maximum marker intensity level. Lastly fig2e shows geodesic dilations iterated until stability, of marker fig2a conditioned on mask fig2b, (the definition of reconstruction by dilation). The seeded region is retained while neighbouring regions are suppressed.

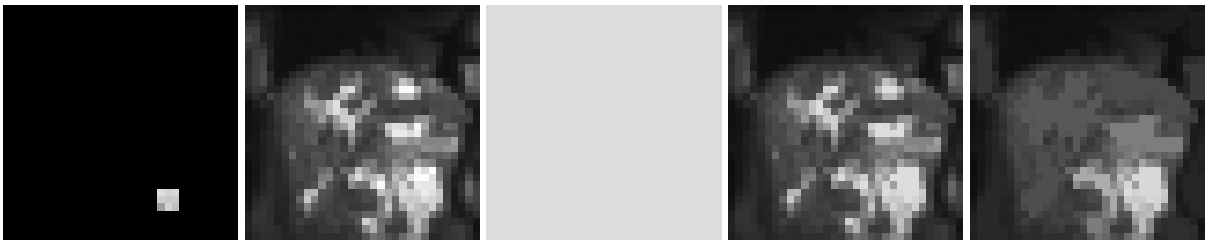

(a) Marker (b) Mask (c) Unconditional (d) Conditional (e) Geodesic

Figure 2: A comparison of standard, conditional, and geodesic dilation using an elementary two dimensional, eight connected structuring element, iterated until stability.

2.2 Hybrid reconstruction

As the caption in Figure 2 states the structuring element used in this example is an elementary two dimensional, eight connected structuring element. If the extents of the structuring element used in the dilation process reach beyond the innermost shell of sample points surrounding the origin the filter is no longer geodesic and cannot be used to perform reconstruction by dilation in the strictest sense of its definition. The procedure would amount to the application of more than one elementary dilation for

each application of the minimum operator (see Eq. 4). The manipulation of structuring elements is an important topic in this field [3, 5, 9], and proves valuable in the development of our procedure here.

$$\delta_C^{h(N,n)} I \;\widehat{=}\; \delta^{(n)} I \wedge C \ldots N \; times \tag{4}$$

This hybrid reconstruction of Eq. 4 has the potential to achieve the behaviour which we wish to utilise in our reconstruction approach, as it will allow the dilation to extend beyond small regions of intensity dropout, without breaching the more extensive low intensity valleys between disconnected neighbouring regions. The more dilations applied per application of the point-wise minimum operator, the wider the gaps which the reconstruction can cross. Thus we can see that there exists a family of reconstructions for any given starting data, where the optimal solution can be chosen in terms of how much physical separation exists at the point of closest proximity between seeded and unseeded regions in the data. So long as this measure allows sufficient scope to bridge the gaps in the fine branch components of the seeded regions, the reconstruction gaol can be successfully achieved.

2.3 Experimental procedure

We applied our approach to the isolation of a network of fine ducts in volumetric medical imaging data used to assess a region of the body in and around the liver. This network, called the biliary tree, collects bile produced in the liver, and delivers it to the small intestine where it is used in the digestive process. Figure 3 shows an example of one of the volumetric datasets under examination: the three dimensional data has been rendered in maximum intensity projection to illustrate the various regions visible, including the biliary tree which we wish to isolate and other structures which are to be suppressed. Note the many constrictions and signal voids visible in the branches of the tree. The ultimate goal of this work is to assist the radiologist in assessing the condition and operation of this ductal network. To this end we wish to achieve a clear and unobstructed reconstruction of the tree in order to facilitate its easy and effective examination and assessment.

We applied both standard reconstruction by dilation using 6, 18, and 26 connected structuring elements (the three fundamental three dimensional structuring elements leading to geodesic reconstructions), and we also applied a series of reconstructions utilising larger structuring elements. These larger elements were constructed so as to achieve approximately isometric reconstruction on the non-isometric volume data which we are analysing. The data is isometric in the x and y directions, with voxel dimensions of approximately 1.3mm each way, but in the z direction the voxel dimensions increase to 4.0mm. Thus in order to achieve dilation more consistently in all directions an anisotropic (in voxel terms) approach was preferred, so as to compensate for the non-cubic nature of the data. We found this to be the most effective approach, maximising the amount of unconstrained dilation we could use between applications of the minimum operator before the procedure starts to include unwanted structures in the reconstruction.

3 Results

We processed a number of datasets using both traditional geodesic reconstruction by dilation and our hybrid reconstruction approach applied at varying strengths, and assessed the reconstruction results achieved in each case. Figure 4 illustrates the superior intensity preservation characteristics of the hybrid reconstruction approach in the processing of objects of interest which include fine branching features. The level of retention achieved increases with the strength of the hybrid reconstruction applied.

We applied the series of reconstructions and then measured the degree of intensity suppression in the neighbouring unseeded regions and at the extreme ends of a number of target branches of varying widths within the seeded regions. Figure 4 shows the variations in signal drop-off observed at two different levels of our hybrid reconstruction, along with standard reconstruction by dilation. In this way we were able to demonstrate the enhanced level of reconstruction achieved using large anisotropic structuring

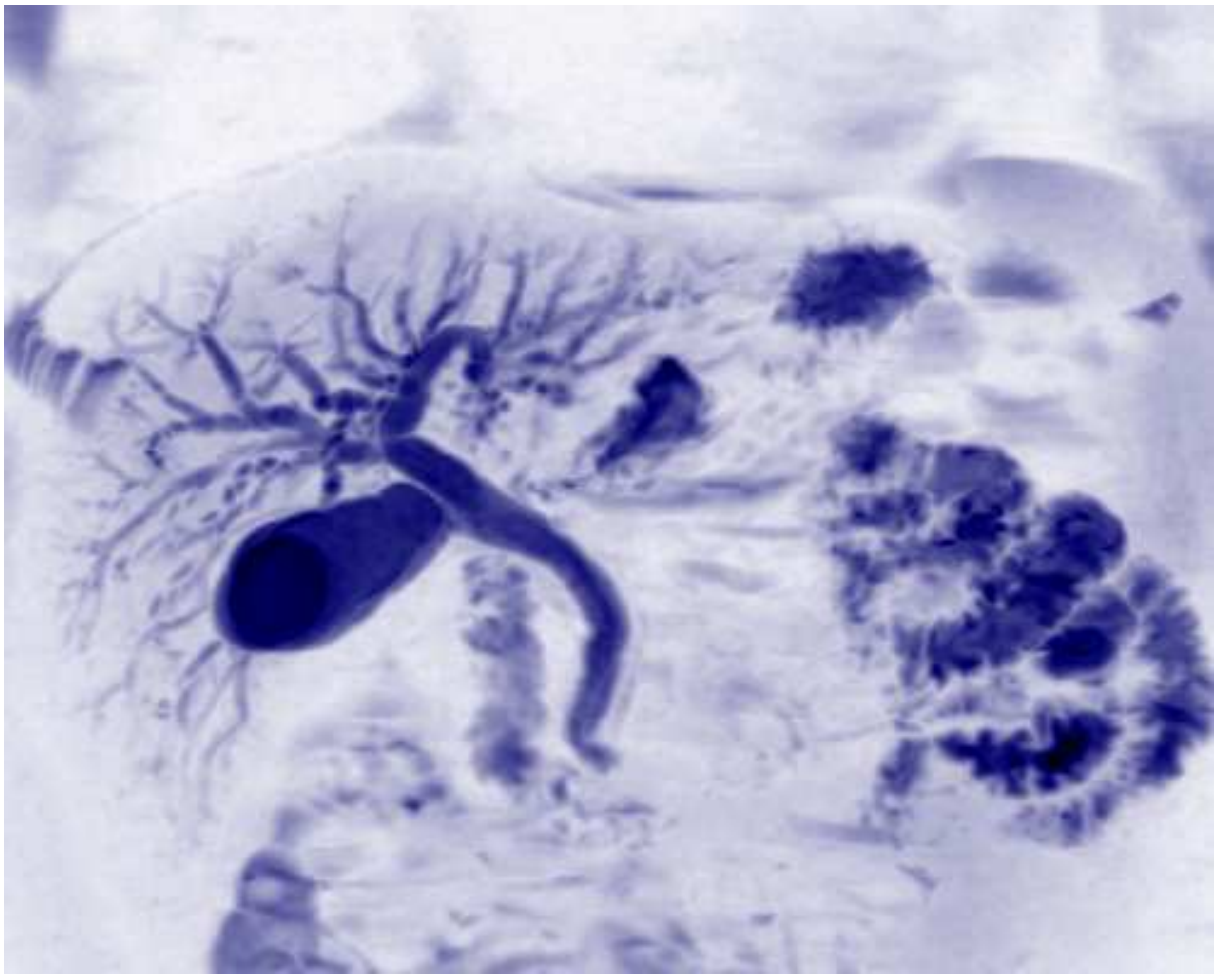

Figure 3: Maximum intensity projection of one of the datasets examined in the study demonstrating the biliary tree along with numerous unwanted high intensity regions.

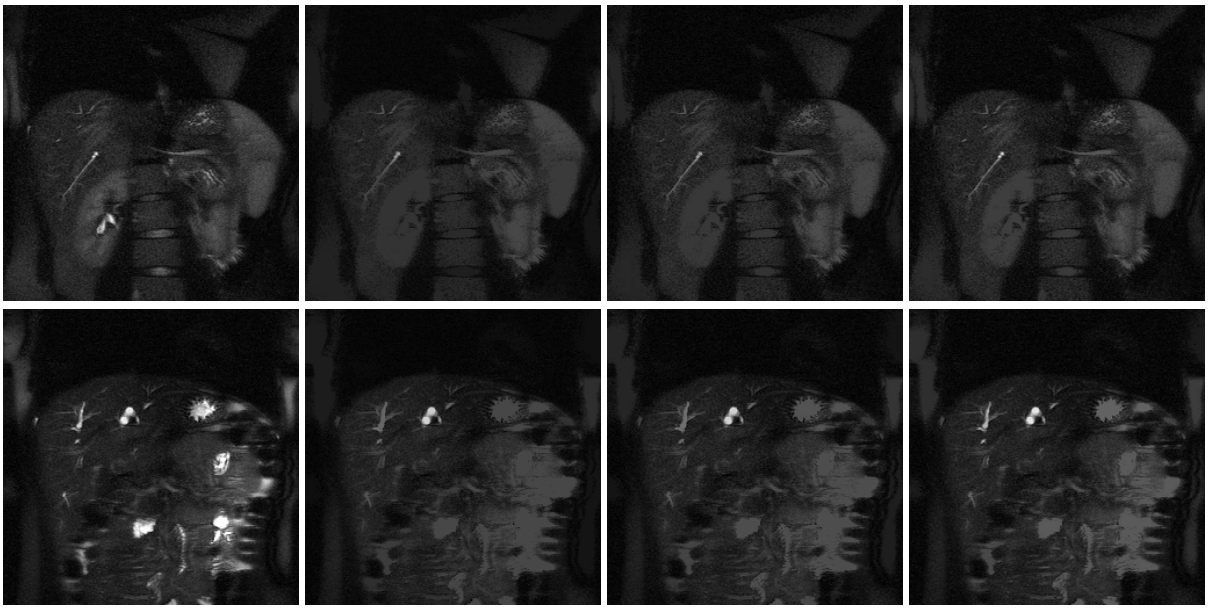

(a) Original (b) Geodesic (c) 38 Anisotropic (d) 54 Anisotropic

Figure 4: Two sections through a volume dataset showing branch tips at various levels of reconstruction demonstrating both fine and course branches: a) original unfiltered data, b) 6-connected geodesic reconstruction by dilation, c) reconstruction using an anisotropic 38 element structuring element, d) reconstruction using an anisotropic 54 element structuring element

elements. Eventually as the size is increased beyond the optimal, the signal intensity in neighbouring regions begins to pick up until in the extreme the reconstruction approximates the original unfiltered data, with only the highest intensity peaks in the data being reduced to the level of the highest intensity sample points present in the original seed data.

In Figure 5 we can in addition observe the enhanced texture retention properties of our hybrid reconstruction approach, where the second row of images achieved using traditional reconstruction by dilation demonstrate excessive smoothing and the introduction of sharp graduations within the reconstructed tree, while the images on row three show superior preservation of the fine detail from the original data (shown on the top row). This can be of particular importance for the accurate interpretation of the final data by the radiologist.

We also observed the role that noise in the data plays in propagating the high intensity signal across background valleys. Once the approach departs from the geodesic scheme where a strict uphill intensity path is always retained between any point and an original seed region, isolated high intensity noise peaks in the background regions have the potential to piggyback the signal across the valleys like a series of stepping stones. This effect makes strong salt and pepper noise particularly unfavourable in the application of our technique. The nature of the noise distribution typical to our data makes the approach more applicable in this case as even with very strong dilations the degree of the unwanted propagation is kept to a manageable level due to the intensity and spatial spread present in the signal noise which means that the maintenance of a high intensity steppingstone path across valleys of any significant width becomes extremely unlikely.

4 Conclusions

By extending the basic principles of reconstruction by dilation beyond the geodesic case we have presented a hybrid reconstruction technique specifically designed to optimally reconstruct objects containing

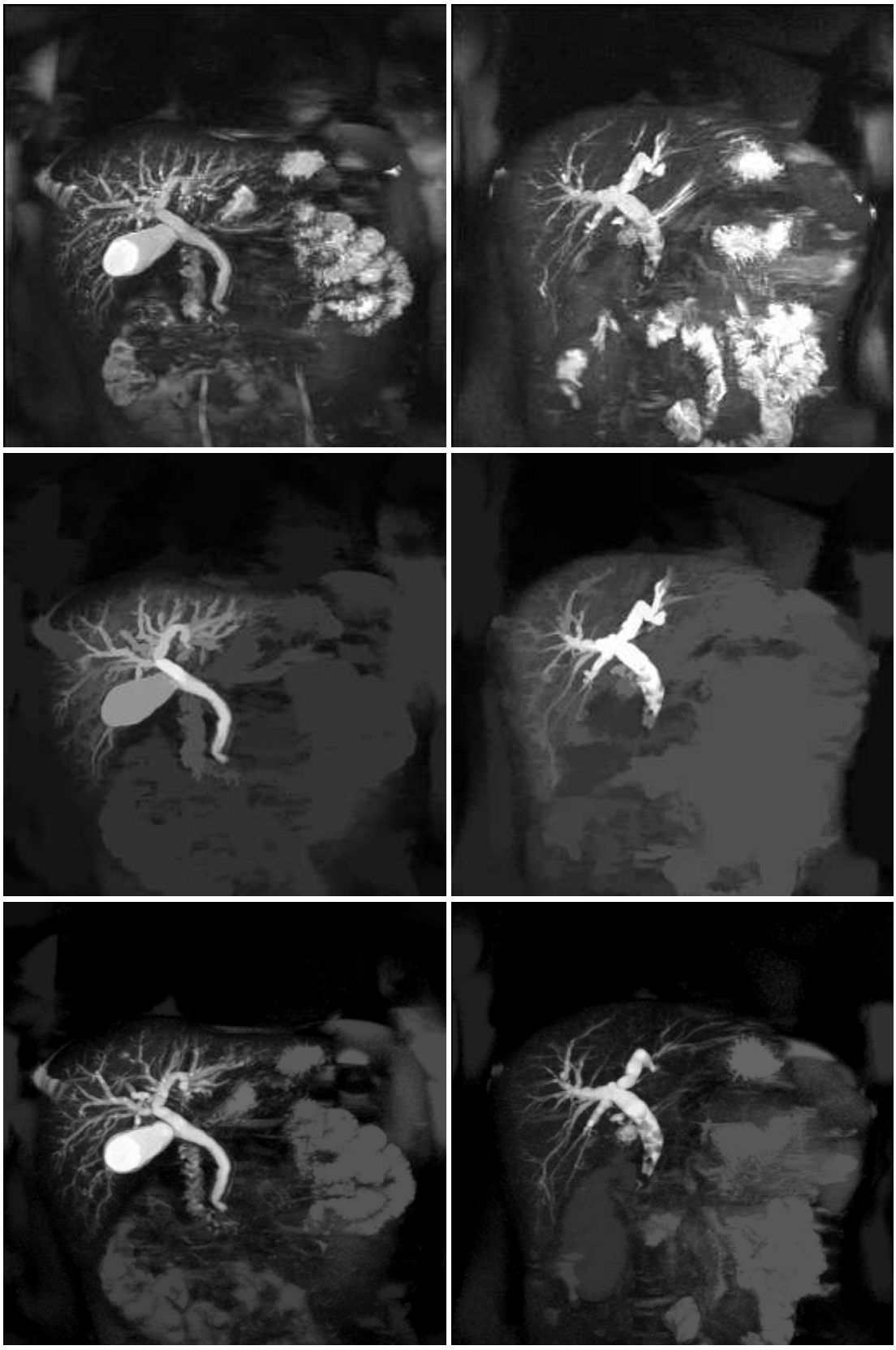

(a) Volume Study 1 (b) Volume Study 2

Figure 5: Maximum intensity projections of two of the datasets from our study, preformed on the original (top row), geodesic reconstructed (middle row), and hybrid reconstructed (bottom row) data volumes.

fine branching structures in the source data while still effectively attenuating the signal from neighbouring unwanted high intensity structures.

Through the application of these techniques we have developed an effective and efficient image processing procedure which yields superior reconstruction results as a precursor to both further automated segmentation, classification, and analysis, and enhanced and simplified manual review of the data by the trained radiologist.

References

[1] J. Angulo and J. Serra. Automatic analysis of dna microarray images using mathematical morphology. *Bioinformatics*, 19(5):553–562, 2003.

[2] A. Araujo, S. Guimaraes, and G. Cerqueira. A new approach for old movie restoration. In *Proc. SPIE-High-speed Imaging and Sequence Analysis*, pages 67–77, 2001.

[3] L. Ji, J. Piper, and J-Y. Tang. Erosion and dilation of binary images by arbitrary structuring elements using interval coding. *Pattern Recognition Letters*, 9(3):201–209, 1989.

[4] V. Metzler, C. Thies, and T. Lehmann. Segmentation of medical images by feature tracing in a selfdual morphological scale-space. In *Proc. SPIE-Medical Imaging*, pages 139–150, 2001.

[5] H. Park and J. Yoo. Structuring element decomposition for efficient implementation of morphological filters. *IEE Proceedings: Vision, Image and Signal Processing*, 148(1):31–35, 2001.

[6] P. Salembier, P. Brigger, J. Casas, and M. Pardas. Morphological operators for image and video compression. *IEEE Transactions on Image Processing*, 5(6):881–898, 1996.

[7] J. Serra. *Image Analysis and Mathematical Morphology*. Academic Press, 1982.

[8] P. Soille. *Morphological Image Analysis: Principles and Applications*. Springer-Verlag, 1999.

[9] M. van Droogenbroeck and H. Talbot. Fast computation of morphological operations with arbitrary structuring elements. *Pattern Recognition Letters*, 17:1451–1460, 1996.

[10] L. Vincent. Morphological grayscale reconstruction in image analysis: Applications and efficient algorithms. *IEEE Transactions on Image Processing*, 2(2):176–201, 1993.